symmetry

MDPI

Article

The Mechanism of Droplet Thermocapillary Migration Coupled with Multi-Physical Fields

Zhijun Ye [1,2], Yi Chen [1], Chao Yang [1], Di Wu [1], Jia Wang [1], Liang Hu [1], Li Duan [1,2,*] and Qi Kang [1,2,*]

[1] National Microgravity Laboratory (NML), Institute of Mechanics, Chinese Academy of Sciences, Beijing 100190, China; yezhijun@imech.ac.cn (Z.Y.)
[2] College of Engineering Sciences, Chinese Academy of Sciences, Beijing 100049, China
* Correspondence: duanli@imech.ac.cn (L.D.); kq@imech.ac.cn (Q.K.)

Abstract: In this paper, the coupling effect of multiphysical fields of droplet migration is deeply studied by constructing a physical model of droplet migration with multiphysical fields. Digital holographic interferometry and particle image velocimetry are used to simultaneously measure the temperature and velocity fields of the mother liquor in the process of droplet migration for the first time. Due to the advancements of measuring, the zero-velocity region is also in the region where the thermal wake appears, four vortexes appear in the droplet migration and the off-axis behavior of double-droplet migration is found. The aim of this work is to analyze the coupling relationship of multiphysical fields, so as to reveal the physical laws of thermocapillary migration of single droplet and multiple droplets with the same phase and heterophase and to study the driving mechanism of the thermocapillary force and the flow of the mother liquor.

Keywords: droplet; thermocapillary migration; multiphysical field; numerical simulation

Citation: Ye, Z.; Chen, Y.; Yang, C.; Wu, D.; Wang, J.; Hu, L.; Duan, L.; Kang, Q. The Mechanism of Droplet Thermocapillary Migration Coupled with Multi-Physical Fields. *Symmetry* **2023**, *15*, 2069. https://doi.org/10.3390/sym15112069

Academic Editor: Mikhail Sheremet

Received: 7 October 2023
Revised: 7 November 2023
Accepted: 10 November 2023
Published: 15 November 2023

1. Introduction

Liquid droplets are commonly found in nature. At the gas–liquid interface of a droplet, the cohesion of molecules generates the interfacial tension, which has a great influence on the behavior of the droplet. In a gravitational field, an independently existing droplet is subjected to the combined effect of gravity and interfacial tension, and can be suspended at the lower end of a water pipe, showing the shape of an ellipsoid. Under microgravity, the morphology of the droplet is different from that in the gravity field. Because the droplet tends to be subjected to zero gravity, it appears to be suspended in the air in the form of a sphere under the action of interfacial tension. The interfacial tension plays an important supporting role to the droplet model, maintaining it in equilibrium, migration, and motion. Microgravity science focuses on the study of the laws of motion of matter under microgravity (low-gravity) environments and the effects of gravity changing on the laws of motion. Microgravity fluid physics has been focusing on the interfacial tension for a long time to carry out research on the process and mechanism of heat and mass transport, especially on the study of secondary processes that are difficult to realize on the ground, as well as on the fluid physics problems associated with manufacturing of materials in space and biotechnology. One of the typical scientific problems in microgravity fluid physics is the thermocapillary migration of droplets. The equilibrium, deformation, vibration and interaction of immiscible droplets in the mother liquor are affected by the liquid–liquid interfacial tension, and the construction of a droplet migration model is scientifically important for the study of interfacial tension mechanism. With the development of microgravity science, droplet dynamics has gradually become a hot spot of research and has a more profound meaning compared to classical fluid mechanics. The study of the droplet thermocapillary migration mechanism has important application value in industries such as space alloy preparation, glass preparation, multiphase separation, crystal growth, droplet combustion and fire safety.

Young, Goldstein and Block [1] proposed the YGB theory in 1959, which initiated the theoretical exploration of droplet thermocapillary migration. In 1990, Barton [2] theoretically analyzed the velocity field and temperature field of droplet thermocapillary migration. For the study of thermocapillary migration of double droplets, Keh [3] theoretically analyzed the thermocapillary migration process of axisymmetric double droplets to obtain the velocity field and droplet migration velocity in the mother liquor.

For the problem of the thermocapillary migration of droplets, research work mostly focuses on numerical simulation. Brady [4] analyzed the thermocapillary migration process of three-dimensional deformable droplets and found that the shape of the cell wall ultimately affects the droplet migration process. Loewenberg [5] calculated the thermocapillary migration velocities of two axisymmetric droplets with different radius ratios. Berejnov [6] gave the evolution of the center distance between two drops over time and discussed the thermocapillary migration process and the interaction of two drops with different radius ratios. Yin [7,8] investigated the thermocapillary migration process of a single droplet with no deformation and discussed the influences of dimensionless parameters and initial conditions on the migration, and also investigated the thermocapillary migration of a two-droplet pair with different radius ratios and the interaction between the two droplets, and analyzed the migration velocities of the large succeeding droplet and the small leading droplet.

Compared with theoretical studies and numerical simulations, there are fewer experiments related to droplet migration. Barton [9] found that the migration rate is proportional to the droplet radius in the experiments of single-droplet thermocapillary migration, which is the same trend predicted by the YGB theory. Hähnel [10] observed the process of large droplets overtaking small droplets in the experiments of double-droplet thermocapillary migration. Our project team, Kang et al. [11] experimentally investigated the thermocapillary migration of two droplets and the interactions between them, and found that the small leading droplets appeared to migrate in an inclined "8" trajectory. In recent years, Kang et al. [12,13] observed the migration processes of single and double droplets in real time using digital holographic interferometry. They discussed the thermal wake problem, analyzed the relationship between the droplet thermocapillary migration velocity and the temperature field around the droplet, and revealed the physical law of the same-phase two-droplet thermocapillary migration and interaction; they carried out the experiment of coaxial three-phase two-droplet thermocapillary migration, observed that the small droplet surpassed the large droplet, and explored the influence of the viscosity coefficient between two droplets of different phases on the migration. Vincent and Delville [14] experimentally studied the thermocapillary migration of the growing droplet in the microchannel by limiting the front advance of the growing droplet by local laser, and found that the laser can control the flow of the droplet in the microchannel, acting as a "soft door". Vikas Chaurasiya et al. [15] explored a mathematical model which accounts for the effect of convection in the frozen and vapor regions, addressed gaps in the modeling of sublimation of a humid porous body. For a specific form of the velocity profile, an exact solution of the current problem is obtained via similarity technique.

Based on the above work, in this paper, we construct a physical model of droplet migration in various multiphysics fields, build a synchronized measurement platform of digital holographic interference and particle image velocimetry, and observe the thermocapillary migration process of a droplet in a temperature gradient field in real time, so as to study the mechanisms that involved multiphysics coupling from a completely new viewpoint. Simultaneous measurements of temperature and velocity fields of single-droplet migration, same-phase two-droplet migration and different-phase two-droplet migration have been conducted. Not only has the droplet thermal wake been observed, but also a region with a zero-velocity field at the rear of the droplet, four vortex cell structures, and the off-axis behavior in two-droplet migration have been discovered for the first time. Numerical simulations of droplet migration have been carried out, and the results of the simulations are in line with those of the experiments. The driving mechanism of droplet migration by

the thermocapillary force and mother liquor flow is explored, and the coupling correlation between the temperature field and velocity field during the droplet migration process as well as the influence factors on the droplet migration state are analyzed.

2. Droplet Migration Model and Measurement Platform

2.1. Droplet Migration Model

Based on the principles of the single-droplet migration model, the same-phase two-droplet migration model and the different-phase two-droplet migration model are shown in Figure 1. We constructed an experimental model that can be used to carry out a variety of droplet migration studies, as shown in Figure 2. The inner cavity of the liquid pool is 40 mm × 40 mm × 70 mm. The liquid pool has four walls of K9 optical glass, and top and bottom plates made of aluminum, with a number of injection holes on the bottom plate; the top plate is heated by an electric heating film, and the bottom plate is cooled by a semiconductor refrigeration plate; the program is written in Labview to ensure a constant temperature gradient in the mother liquor. The density-matching method is used to reduce the buoyancy effect caused by gravity to study the droplet thermocapillary migration. The 30 cSt silicone oil is selected as the mother liquor, and the glycerol–ethanol and water–ethanol mixtures are used as the droplet liquid to realize the single-droplet migration, the same-phase two-droplet migration, the different-phase two-droplet migration, and so on. The ratio of the droplet diameter to the width of the mother liquor is defined as Ar = d/W, where d is the droplet diameter and W is the width of the mother liquor (the width of the liquid pool). Physical parameters are shown in Table 1.

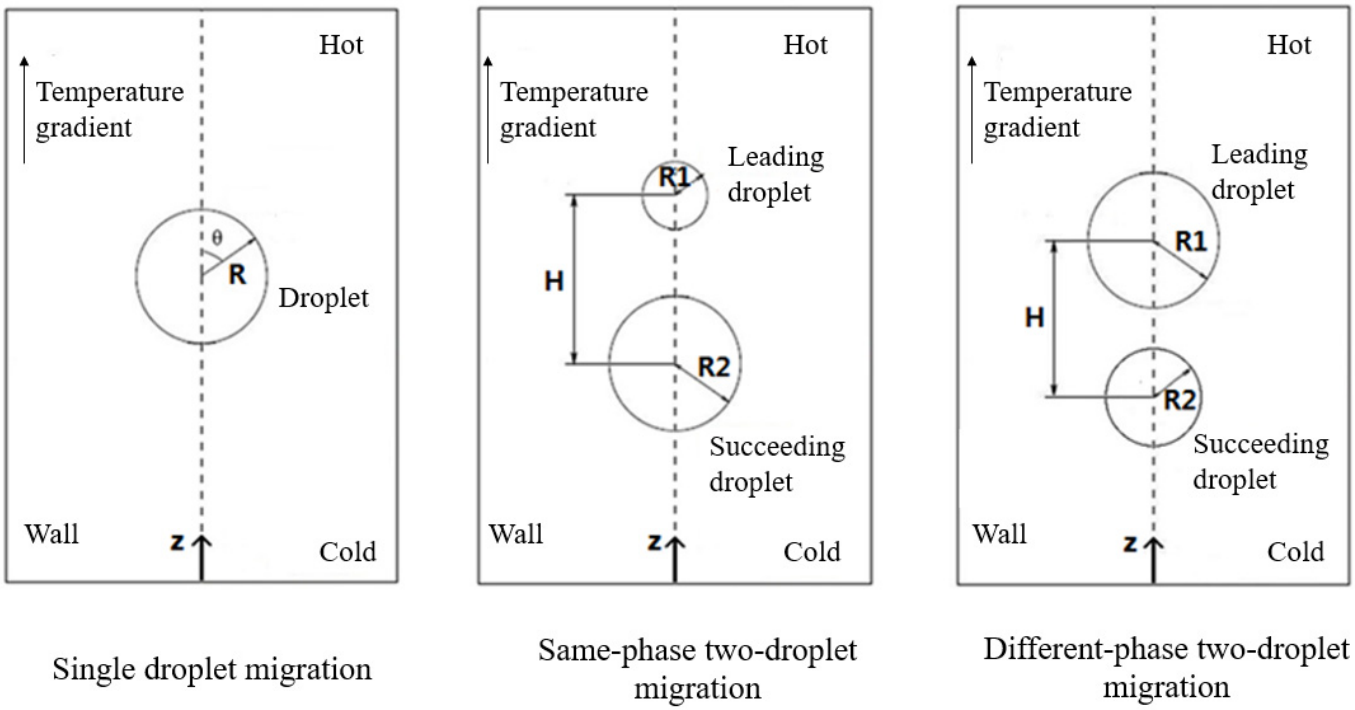

Figure 1. Physical model of droplet migration.

Table 1. Physical Parameters.

	ν/ ($\mu m^2 \cdot s^{-1}$)	ρ/ ($kg \cdot m^{-3}$)	Λ/ ($W \cdot m^{-1} \cdot K^{-1}$)	σ_T/ ($\mu N \cdot m^{-1} \cdot K^{-1}$)
30 cSt silicone oil	30.0	955	0.151	
Glycerol–ethanol mixture	8.7	955	0.20	−50.4
Water–ethanol mixture	2.8	955	0.41	−86.3

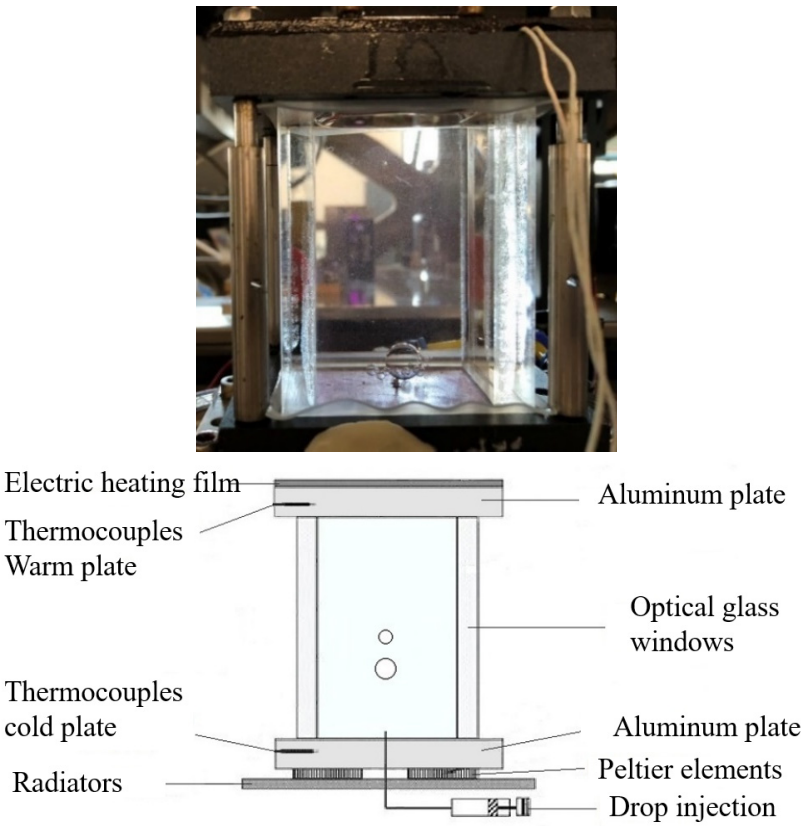

Figure 2. Experimental model system.

2.2. Measurement Platforms

The major difference between this paper and the previous work lies in the synchronized measurements of velocity and temperature fields during the droplet migration and interaction process to explore the multiphysics field coupling mechanism. Based on the development of the fluid physics experimental cabinet on the space station, a synchronized optical measurement platform of particle image velocimetry and digital holographic interferometry thermometry is constructed to carry out the research on the multiphysics field coupling of liquid droplet migration.

Particle image velocimetry, referred to as PIV, has been a mature technique and advanced products are available since its inception in the 1980s. But due to the need for simultaneous measurements of the velocity field and the temperature field in this study, we built our own optical system based on the basic principles of PIV. The basic principle of PIV is that the flow field filled with tracer particles is illuminated by the slice of light formed by the laser through a column lens, and the image is continuously captured twice or multiple times by a CCD camera to obtain the PIV film, as shown in Figure 3. The product correlation algorithm (Equation (1)) is usually used in the image processing, combined with the normalization method (Equation (2)); the image recognition can be achieved to obtain the magnitude and direction of the velocity of the flow field.

$$R(k,l) = \sum_{m=0}^{m_{a-1}} \sum_{n=0}^{n_{a-1}} x(x,y)y(m+k,n+l) \tag{1}$$

$$\rho(k,l) = \frac{R(k,l)}{\sqrt{\sum_{m=0}^{m_{a-1}} \sum_{n=0}^{n_{a-1}} x^2(x,y)} \sqrt{\sum_{m=0}^{m_{a-1}} \sum_{n=0}^{n_{a-1}} y^2(m+k,n+l)}} \tag{2}$$

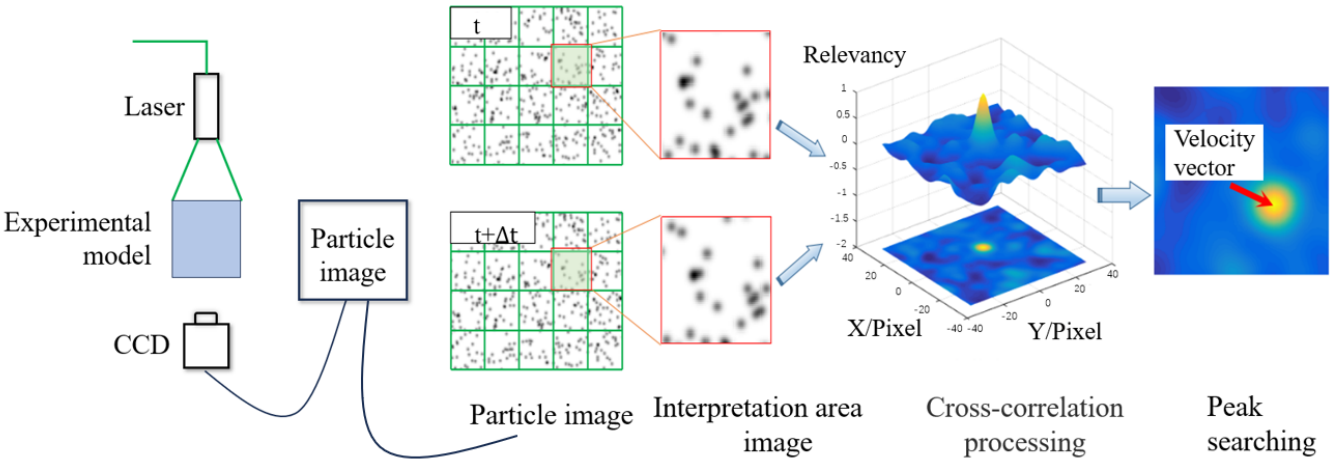

Figure 3. Particle image velocimetry technology (PIV).

The digital holographic interferometry System (DHI) utilizes digital holographic interferometry based on the principle of secondary exposure to record holograms by a CCD camera instead of a holographic dry plate, and realizes the reconstruction of the object field to be measured by numerically reproducing the changing object field through a computer. DHI provides an important experimental approach for the study of dynamic behavior of complex flow fields. Digital holographic interferometry has many advantages, for example, it allows for a full-field measurement; the measurement process is noncontact, and will not affect the flow field; real-time detection can be carried out, and various instantaneous states of the flow field can be recorded directly; quantitative measurements and analyses can be obtained with high precision and high sensitivity.

The optical path of the digital holographic interferometry (DHI) system is shown in Figure 4, and the numerical reconstruction is shown in Figure 5. The laser beam generated by the laser is transmitted through an optical fiber, which reduces the influence of external noise on the light source. The laser source is divided into a beam of object light and a beam of reference light by the fiber coupler. The object beam is transmitted through the experimental fluid after beam expansion and collimation. Due to the temperature gradient in the experimental mother liquor, the refractive index distribution in the mother liquor is heterogeneous, which results in the corresponding modulation of the phase distribution of the wavefront of the object light, and this modulation changes with the refractive index distribution of the fluid. The transmitted object beam passes through the 4f system and then is projected onto the photosensitive surface of the CCD camera through a beam-splitting prism. The reference beam, after beam expansion and collimation, is projected onto the photosensitive surface of the CCD camera through a beam-splitting prism. As it interferes with the modulated object beam, the hologram is formed. The CCD records the holograms of the mother liquor in different states and obtains the phase changes of the object beam in different states through numerical reconstruction, thereby obtaining the changes of refractive index. The complex amplitude of the light received by the CCD target can be obtained through Equation (3); the intensity of the light received by the CCD target can be obtained through Equation (4). The spatial spectrum of the hologram can be obtained by Fourier transform of the light intensity distribution. Among G_1, G_2, G_3 and G_4, G_3 and G_4 are the ± 1 level spectra of the object light, respectively. After extracting G_3 or G_4, the inverse Fourier transform can be used to obtain the object light on the hologram plane. The temperature distribution in the mother liquor in the corresponding state is then deduced from the relationship between refractive index and temperature.

$$\mathrm{U}(x_\mathrm{H}, y_\mathrm{H}) = r\exp(-\mathrm{j}2\pi\xi_\mathrm{r}x_\mathrm{H}) + u_\mathrm{H}(x_\mathrm{H}, y_\mathrm{H}) \quad (3)$$

$$i_{\mathrm{H}}(x_{\mathrm{H}}, y_{\mathrm{H}}) = r^2 + \left|u_{\mathrm{H}}(x_{\mathrm{H}}, y_{\mathrm{H}})\right|^2 + r u_{\mathrm{H}}(x_{\mathrm{H}}, y_{\mathrm{H}}) \exp(\mathrm{j}2\pi\xi_r x_{\mathrm{H}}) + r u_{\mathrm{H}}^{*}(x_{\mathrm{H}}, y_{\mathrm{H}}) \exp(-\mathrm{j}2\pi\xi_r x_{\mathrm{H}}) \quad (4)$$

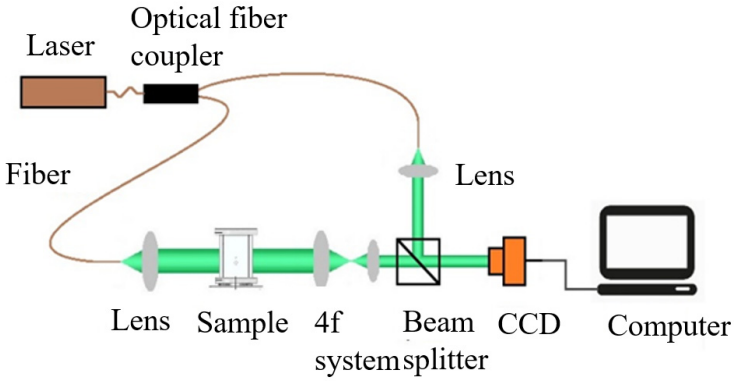

Figure 4. Digital holographic interferometry system principle.

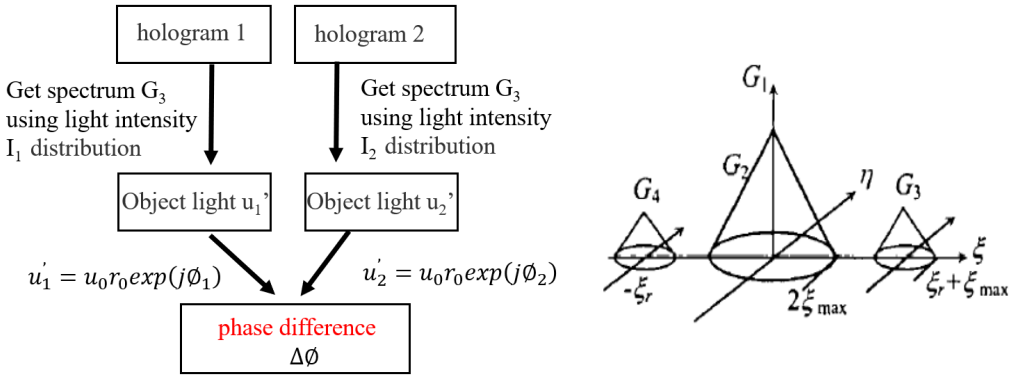

Figure 5. Numerical reconstruction.

Based on the basic principles of particle image velocimetry (PIV) and digital holographic interferometry (DHI), a platform for simultaneous measurements of velocity and temperature fields is constructed, and the schematic diagram and the physical layout are shown in Figures 6 and 7 respectively. The digital holographic interference system (DHI) uses laser 2 with a wavelength of 532 nm and a power of 50 mW to output a laser beam which is transmitted to an optical platform through an optical fiber. The laser beam passes through a lens set to form a parallel beam with a beam aperture greater than 50 mm. After this parallel beam passes through the experimental section and the lens group, an object beam with a beam aperture of less than 15 mm that matches the size of the CCD target is formed through the beam-splitting prism. The object beam meets the reference beam and forms an interferogram that is recorded by the large-area array CCD. The phase map is reconstructed from the hologram and the physical field distribution is obtained. The particle image velocimetry (PIV) system uses laser 1 with a wavelength of 561 nm and a power of 150 mW to output a laser beam which is transmitted to an optical platform through an optical fiber. The laser beam passes through a column lens to form a slice of laser light, illuminating a cross section of the experimental section; a sequence of particle images characterizing the fluid structure are recorded by a high-speed CCD camera with a filter installed in front of the camera, and the filter has the same output wavelength as laser 1; then the information such as the velocity distribution of the flow is obtained through the correlation processing of the particle images.

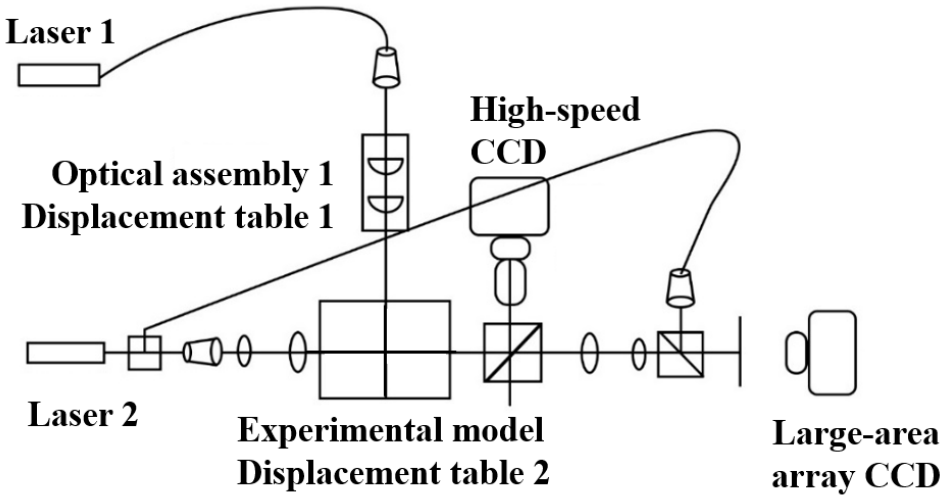

Figure 6. Schematic diagram of measuring platform.

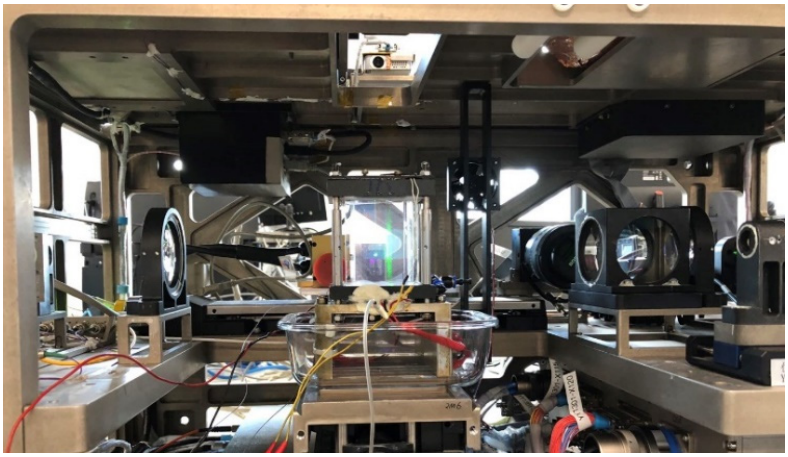

Figure 7. Physical diagram of the measurement platform of the fluid physics experiment cabinet of the space station.

3. Results and Analysis of Droplet Migration Experiments

3.1. Principle of Droplet Thermocapillary Migration

The droplet migration problem is a complex process driven by the coupling of multiple physical fields. The droplet is submerged in another immiscible mother liquor, and a temperature gradient is added to the mother liquor, which causes the temperature inhomogeneity at the droplet interface and leads to the inhomogeneity of the interfacial tension, thus driving the flow of the fluids on both sides of the interface, and the droplet will move due to the reaction force of the shear stress of the mother liquor, which is called the thermocapillary migration of the droplet. Previous studies have concluded that in the process of droplet thermocapillary migration, convective cell elements are formed inside the droplet, and the around-flow is formed outside the droplet, as shown in Figure 8. We have obtained results that are different from this conclusion by simultaneous measurements of the velocity field and the temperature field during the droplet migration process, and have gained a brand new understanding of the process of droplet migration.

The Maragoni number (hereafter referred to as Ma number) represents the ratio of thermal convective transport to thermal diffusion and is defined as follows:

$$\mathrm{Ma} = \frac{|\sigma_T|\Gamma R^2}{\rho \nu \kappa} \tag{5}$$

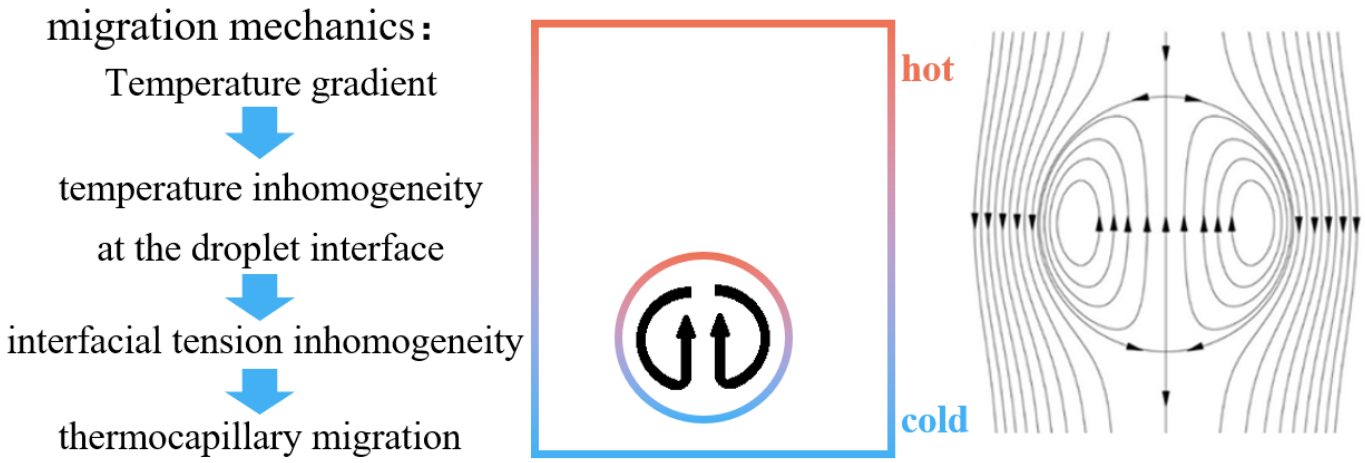

Figure 8. Principle of droplet thermocapillary migration.

3.2. Single-Droplet Migration

In the experiment of single-droplet migration in a uniform temperature gradient field, the mother liquor is 30 cSt silicone oil and the droplet is a mixture of water and ethanol to ensure density matching. The temperature gradient of the mother liquor Γ = 0.57 K/mm, d = 6 mm, Ar = 0.15, Ma = 1.62×10^3. The droplet migration temperature and velocity fields are observed in real time using a synchronized measurement platform developed in this study.

The hologram at t = 0 and the hologram at a certain moment in the droplet migration process are collected, and the original holograms are processed to obtain the phase distribution map that reflects the temperature field distribution and the temperature field distribution (unwrapped phase map) at the corresponding moments, as shown in Figure 9. Throughout the whole process of droplet migration, from the digital holographic interferometric measurements, it is found that there exists a thermal boundary layer near the interface of the droplet, and the droplet tail appears as a thermal wake.

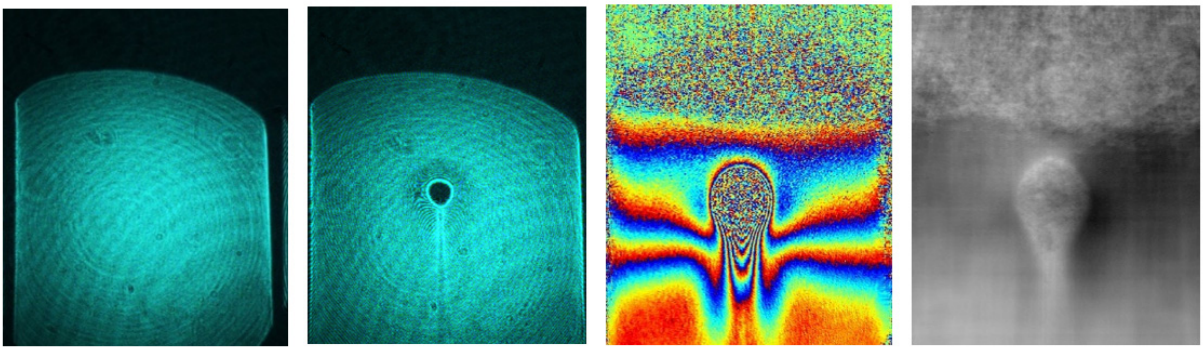

Figure 9. Hologram, phase diagram (different colors mean different phases), and temperature field distribution.

The droplet is surrounded by a low-temperature zone, where the temperature around the droplet is lower than in the mother liquor of the same height, and a thermal boundary layer exists. The main reason is because the effect of convective transport is strong. In the experiment, the Ma number is large, and the thermal convection effect is relatively strong, while the thermal conduction effect is relatively weak. The droplet will migrate to the high-temperature end due to the thermocapillary effect, and the droplet will have a lower temperature than the surrounding mother liquor. However, the heat used to increase the internal temperature of the droplet is mainly supplied by the mother liquor through thermal conduction, rather than through thermal radiation and thermal convection. This

heat transfer mechanism results in a relatively weak heat exchange between the interior and exterior of the droplet. This ultimately results in a temperature difference between the interior and exterior of the droplet. A thermal boundary layer exists near the droplet interface to maintain the continuity of heat flux.

The presence of thermal wake can also be observed clearly at the rear of the droplet. The actual temperature isotherms at the rear of the droplet are bent, neither straight nor symmetrical with respect to the horizontal axis passing through the droplet center, which is mainly due to the thermal convective transport. The droplet affects the surrounding temperature field, and the droplet migration bends the isotherms of the originally flat background temperature field. In the vicinity of the front stationary point of the droplet, the isotherms are bent to the high-temperature end, and the isotherms are gathered near the front stationary point of the droplet, which makes the temperature gradient increase in the mother liquor near and above the front stationary point; in the vicinity of the rear stationary point of the droplet, there exists a long thermal wake at the rear of the droplet, and the isotherms are more sparse in the region of the thermal wake below the rear stationary point of the droplet, which makes the temperature gradient smaller in the mother liquor near and below the rear stationary point.

The coupling between the velocity field and temperature field during the droplet migration process is investigated, and the results of the simultaneous PIV measurements are shown in Figure 10. It is found that the phenomena of boundary layer and wake also exist in the velocity field, and the PIV results are consistent with the digital holographic interferometry results. The complex temperature field in the region of the droplet thermal wake in turn leads to a region with a zero-velocity field at the rear of the droplet, a result that is new to us and has not been reported in previous studies. The temperature field is strongly coupled with the velocity field during the droplet migration process. The interfacial tension drives the flow of mother liquor to generate the velocity field, the velocity field causes the temperature field to change, and the temperature field acts on the droplet migration, resulting in a complex structure of temperature field and flow field. This complex structure has a direct impact on the droplet migration state, affecting the equilibrium of the droplets and leading to migration instability.

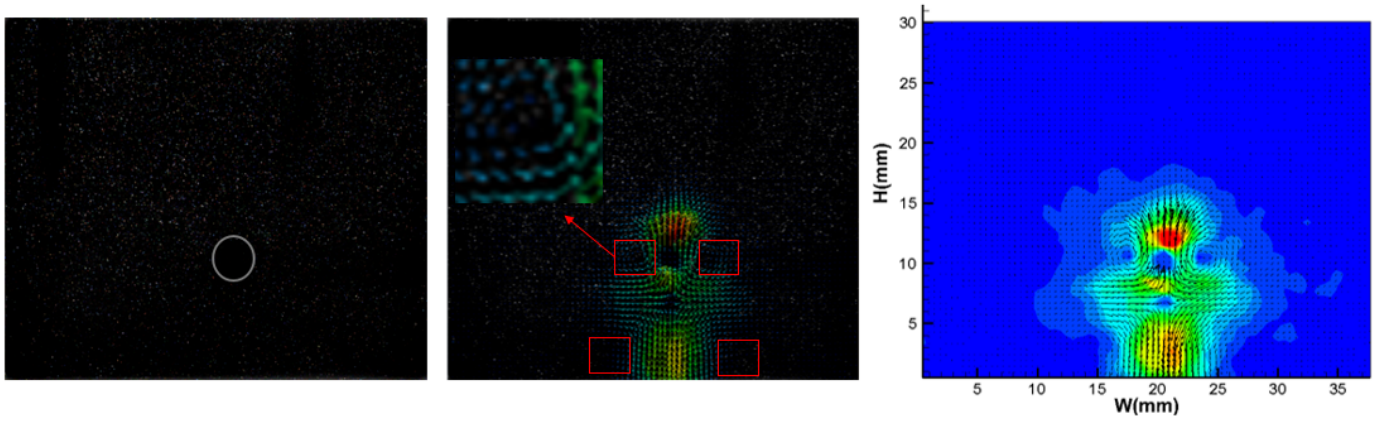

Figure 10. Particle image (white circle is to show the droplet) and velocity field distribution (different colors mean different velocity) of droplet migration process.

In addition to the phenomena of thermal boundary layer, thermal wake, velocity boundary layer and velocity wake, a new understanding of the flow field structure is obtained. Four vortex cells are found to be distributed in the mother liquor during the thermocapillary migration process of a single droplet in the experiments of simultaneous measurements of temperature field and velocity field, as shown in Figure 11. Two larger vortex cells exist in the mother liquor above the droplet, and two smaller vortex cells exist in the mother liquor in the tail region of the droplet, which is consistent with the results of numerical simulation. This is different from the previous results (see Figure 8), and

the coupling between the temperature field and velocity field in the droplet migration process should be investigated to re-recognize and explore the mechanism of surface tension effect of droplet migration. Previous theoretical studies have mainly investigated the thermocapillary behavior of droplets in an infinite flow field, but in a finite flow field, the boundary conditions of the flow field affect the flow of mother liquor. When the droplet moves vertically upward driven by the thermocapillary force, the mother liquor around the droplet also moves upward with the droplet, and due to the finite flow field and the conservation of mass of the mother liquor, the mother liquor farther away from the droplet moves downward, so a region in the mother liquor with zero velocity appears inside the droplet wake region. And the position of this region of zero velocity continues to move upward in the process of droplet migration. When the region is farther away from the wall of the liquid pool, the horizontal velocity of the mother liquor is no longer zero, and there is vertical motion in the mother liquor in the opposite direction at this time; the vortex cells in the mother liquor begin to form in the region of the droplet tail.

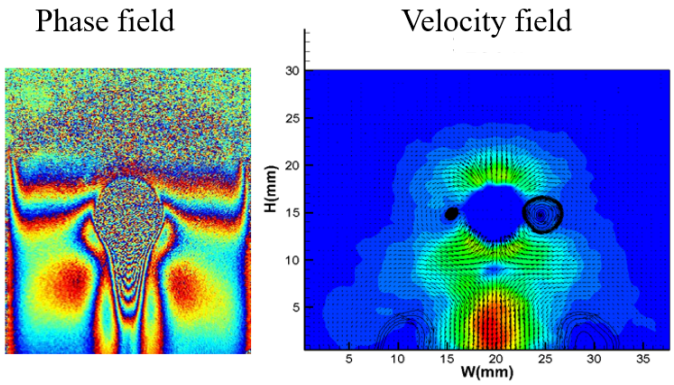

Figure 11. Phase field (different colors mean different phase) and velocity field (different colors mean different velocity) of droplet migration process.

3.3. Same-Phase Two-Droplet Migration

In the experiment of same-phase two-droplet migration in a uniform temperature gradient field, the temperature gradient is 0.57 K/mm. The leading droplets of 7 mm diameter are injected into the mother liquor first, and then the succeeding droplets of 7.8 mm diameter are injected afterwards. $Ma_{lead} = 2.20 \times 10^3$, and $Ma_{suc} = 2.74 \times 10^3$. Since the diameter of the succeeding droplet is relatively large, according to the YGB theory, the migration velocity of the droplet increases with the increase in the diameter, so the migration velocity of the succeeding droplet is faster than that of the leading droplet, and the process of the succeeding droplet catching up with the leading droplet can be observed in the experiment. Through the analysis of the velocity field and the corresponding phase field, it is found that the large succeeding droplet will cause the deviation of the small leading droplet from the axis of the succeeding droplet during the process of chasing; when the deviation between the two droplet axes is large, the phase field will be changed from the axisymmetric state to the asymmetric state; the asymmetric temperature field causes the two droplet axes to continue to shift, as shown in Figure 12. The reason for this phenomenon is that the two-droplet migration has a more complicated temperature field structure and flow field structure, which leads to the oscillation of droplet migration, and the double-droplet migration deviates from the coaxial motion.

From the initial phase field, it can be seen that the initial temperature field has a vertical uniform temperature gradient. When the succeeding droplets are farther away from the leading droplets, the temperature gradient in the mother liquor is still relatively uniform; when the succeeding droplets are about to catch up with the leading droplets, the direction of the temperature gradient in the mother liquor is obviously tilted. The tilted temperature gradient leads to the tilt of the surface tension gradient; as a result, the direction of the surface tension on the droplets will change. Since the diameter of the succeeding droplet

is larger than that of the leading droplet, the migration velocity of the succeeding droplet is greater than that of the leading droplet, and it can be seen from Figure 12a,b when the temperature field appears to be tilted, the velocity field of the mother liquor around the surfaces of the two droplets is also tilted. Regions of zero velocity are found inside the droplet wake region in both the two-droplet migration and single-droplet migration.

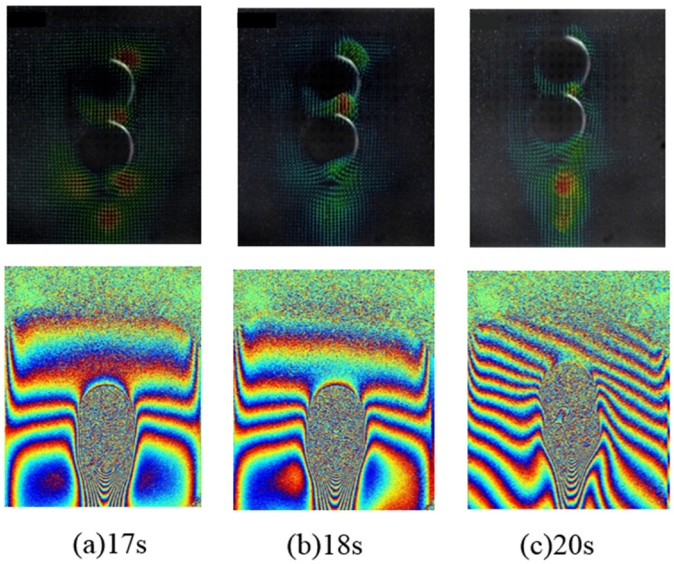

Figure 12. Same-phase two-droplet migration velocity fields (different colors mean different velocity) and phase fields (different colors mean different phase).

3.4. Heterophase Two-Droplet Migration

In the experiment of different-phase two-droplet migration in a uniform temperature gradient field, the temperature gradient is 0.57 K/mm. A leading droplet with a diameter of 8 mm and a glycerol–ethanol mixture (ν = 8.7) as the working medium is injected into the mother liquor first, and then a succeeding droplet with a diameter of 3.8 mm and a water-ethanol mixture (ν = 2.8) as the working medium is injected into the mother liquor afterwards. $Ma_{lead} = 1.11 \times 10^3$, and $Ma_{suc} = 6.50 \times 10^2$. According to the YGB theory, the droplet motion velocity is proportional to the droplet diameter and inversely proportional to the liquid viscosity. In this working condition, the velocity of the small succeeding droplet is greater than that of the large leading droplet, and the small succeeding droplet will chase and overtake the large leading droplet. It is found in this process that when the small succeeding droplet overtakes the large leading droplet, the moving directions of both the small succeeding droplet and the large leading droplet are tilted, as shown in Figure 13.

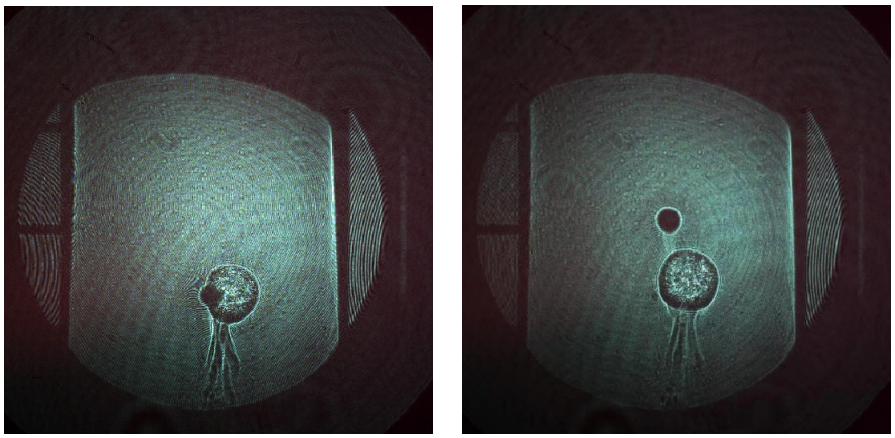

Figure 13. Hologram of different-phase two-droplet migration.

4. Numerical Simulation Results and Analysis

Numerical simulations of the single-droplet thermocapillary migration flow field are performed using a dynamic mesh method and no-slip boundary condition. Dynamic mesh method is a multiphysics interface designed to model laminar two–phase flow of immiscible fluids separated by a moving interface. The focus is on the droplet migration process. The temperature gradient of the mother liquor causes the interfacial temperature gradient between the mother liquor and the droplet, which leads to the interfacial tension gradient, driving the flows of the intradroplet fluid and the mother liquor, thus causing droplet migration, as shown in Figure 14. Boundary conditions exist in the mother liquor, which have a large impact on the flow of the mother liquor and the behavior of the droplet. During the upward migration of the droplet, the velocity of the mother liquor is zero at the boundary, and the velocity of the mother liquor around the droplet is the same as the droplet velocity. Due to the mass conservation of the mother liquor, the moving direction of the mother liquor farther away from the droplet is opposite to the moving direction of the droplet during the migration process, which gradually forms the tail vortex behind the droplet. Numerical simulation results show that four vortex cells are formed in the mother liquor, and the vortex cells in the droplet gradually develop from two to four. This conclusion is the same as our experimental results.

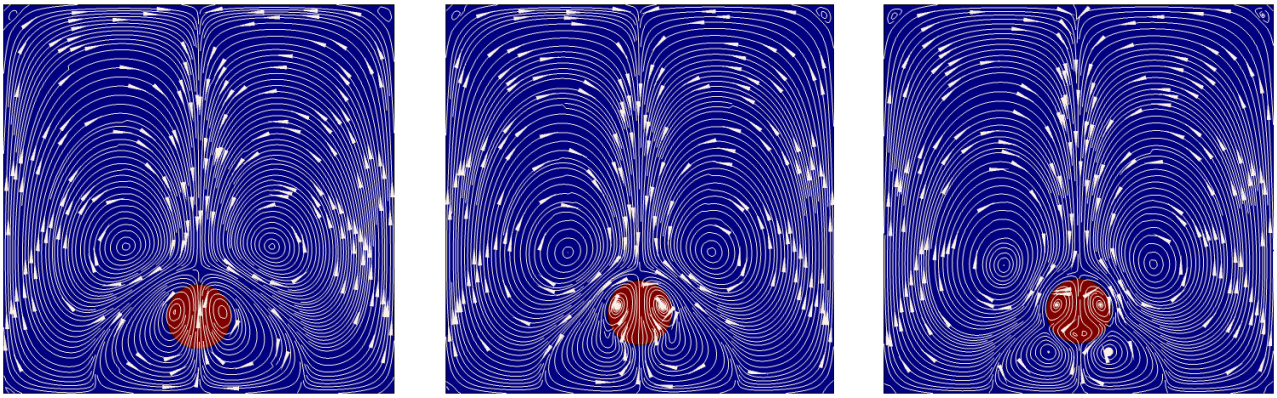

Figure 14. Numerical simulation of droplet thermocapillary migration(streamline is shown in the figure, red circle means droplet).

5. Conclusions

In this paper, we construct a physical model of droplet migration in various multiphysics fields, and set up a synchronized optical measurement platform by using digital holographic interferometry and particle image velocimetry based on the development of the fluid physics experimental cabinet on the Chinese space station, in order to observe the thermocapillary migration of droplets in temperature gradient field in real time, and to study the coupling mechanism of multiphysics fields from a new viewpoint. The temperature and velocity fields of single-droplet migration, same-phase two-droplet migration, and different-phase two-droplet migration are measured experimentally, and the mechanism of droplet thermal wake is discussed and analyzed. By measuring the velocity field of droplet migration, (1) a region with a zero-velocity field at the rear of the droplet is firstly found; (2) four vortex structures are firstly observed and verified by numerical simulation; (3) the off-axis behavior of double-droplet migration are found for the first time. The physical phenomena are analyzed and discussed from the mechanical point of view, and the coupling correlation of multiphysics fields and the influencing factors are analyzed.

The study of droplet thermocapillary migration due to the uniform temperature field is of great significance in revealing the role of thermocapillary force in the interfacial behavior. Liquid rocket combustion systems, space environment cooling systems, and the space welding are among the many applications of space technology that involve droplet thermocapillary migration. In future long-duration space flights, sewage treatment

and food processing in space are issues that astronauts must consider, which involve problems of two-phase or multiphase separation. However, the droplet behavior cannot be manipulated more precisely in this paper, but it still lays theoretical and experimental foundations for the use of thermocapillary force to lead the interfacial behavior.

Author Contributions: Conceptualization, Z.Y.; Software, C.Y.; Validation, Y.C., C.Y., D.W., J.W. and L.H.; Formal analysis, Z.Y.; Investigation, Z.Y. and Y.C.; Resources, L.D. and Q.K.; Writing–original draft, Z.Y; Writing–review & editing, L.D.; Supervision, L.D. and Q.K.; Project administration, L.D. and Q.K.; Funding acquisition, L.D. and Q.K. All authors have read and agreed to the published version of the manuscript.

Funding: This research was funded by the National Natural Science Foundation of China (12072354 and 12032020), the manned space program of China, and the Strategic Priority Research Program on Space Science of Chinese Academy of Sciences.

Data Availability Statement: The data presented in this study are available on request from the corresponding author. The data are not publicly available due to data security.

Conflicts of Interest: The authors declare no conflict of interest.

Nomenclature

Variable name	Physical meaning (of the liquid)	Variable name	Physical meaning
ρ	density	Γ	temperature gradient in the mother liquor
ν	kinematic viscosity coefficient	R	radius of the droplet
μ	kinetic viscosity coefficient	d	diameter of the droplet
κ	thermal diffusion coefficient	σ_T	coefficient of variation of the interfacial tension with the temperature
Λ	thermal conductivity	Ar	ratio of the droplet diameter to the width of the mother liquor

References

1. Young, N.O.; Goldstein, J.S.; Block, M.J. The motion of bubbles in a vertical temperature gradient. *J. Fluid Mech.* **1959**, *6*, 350–356. [CrossRef]
2. Barton, K.D.; Subramanian, R.S. Thermocapillary migration of a liquid drop normal to a plane surface. *J. Colloid Interface Sci.* **1990**, *137*, 170–182. [CrossRef]
3. Keh, H.J.; Chen, S.H. The axisymmetric thermocapillary motion of two fluid droplets. *Int. J. Multiph. Flow* **1990**, *16*, 515–527. [CrossRef]
4. Brady, P.T.; Herrmann, M.; Lopez, J.M. Confined thermocapillary motion of a three-dimensional deformable drop. *Phys. Fluids* **2011**, *23*, 022101. [CrossRef]
5. Loewenberg, M.; Davis, R.H. Near-contact thermocapillary motion of two non-conducting drops. *J. Fluid Mech.* **1993**, *256*, 107–131. [CrossRef]
6. Berejnov, V.; Lavrenteva, O.M.; Nir, A. Interaction of two deformable viscous drops under external temperature gradient. *J. Colloid Interface Sci.* **2001**, *242*, 202–213. [CrossRef]
7. Yin, Z.; Chang, L.; Hu, W.; Li, Q.; Wang, H. Numerical simulations on thermocapillary migrations of nondeformable droplets with large Marangoni numbers. *Phys. Fluids* **2012**, *24*, 092101. [CrossRef]
8. Yin, Z.; Li, Q. Thermocapillary migration and interaction of drops: Two non-merging drops in an aligned arrangement. *J. Fluid Mech.* **2015**, *766*, 436–467. [CrossRef]
9. Barton, K.D.; Subramanian, R.S. The migration of liquid drops in a vertical temperature gradient. *J. Colloid Interface Sci.* **1989**, *133*, 211–222. [CrossRef]
10. Hähnel, M.; Delitzsch, V.; Eckelmann, H. The motion of droplets in a vertical temperature gradient. *Phys. Fluids A Fluid Dyn.* **1989**, *1*, 1460–1466. [CrossRef]
11. Kang, Q.; Hu, L.; Huang, C.; Cui, H.L.; Duan, L.; Hu, W.R. Experimental investigations on interaction of two drops by thermocapillary-buoyancy migration. *Int. J. Heat Mass Transf.* **2006**, *49*, 2636–2641. [CrossRef]
12. Zhang, S.T.; Duan, L.; Kang, Q. Experimental research on thermocapillary migration of drops by using digital holographic interferometry. Exp. *Fluids* **2016**, *57*, 1–13.

13. Zhang, S.; Duan, L.; Kang, Q. Experimental Research on Thermocapillary—Buoyancy Migration. *Microgravity-Sci. Technol.* **2018**, *30*, 183–193.
14. Vincent, M.; Delville, J.P. Thermocapillary migration in small-scale temperature gradients: Application to optofluidic drop dispensing. *Phys. Rev. E* **2012**, *85 Pt 2*, 026310. [CrossRef]
15. Vikas, C.; Ankur, J.; Jitendra, S. Analytical study of a moving boundary problem describing sublimation process of a humid porous body with convective heat and mass transfer. Journal of thermal analysis and calorimetry. *J. Therm. Anal. Calorim.* **2023**, *148*, 2567–2584.